sciendo

Int. J. of Applied Mechanics and Engineering, 2022, vol.27, No.1, pp.67-77
DOI: 10.2478/ijame-2022-0005

FRICTION SPOT LAP JOINING OF ALUMINUM ALLOY AA6061 TO PRE-HOLED AND THREADED CARBON STEEL AISI 1006

H.K. IBRAHIM, S.K. HUSSEIN* and K.J. JADEE
Engineering Technical College - Baghdad, Middle Technical University, Baghdad, IRAQ.
E-mail: sabah.kh1974@yahoo.com

This work addresses to joining aluminum alloy AA6061 to carbon steel AISI 1006 sheets using the friction spot joining technique. The steel sheets were pre-holed and threaded with an internal M6 thread. The joining process was carried out by extruding the aluminum through the steel hole and thread using a rotating tool with friction between the tool and aluminum. Three process parameters were used: pre-heating time, rotating speed and plunging depth of the tool, with four levels for each parameter. The results indicated that the two materials joined by a micro-scale mechanical interlock at an interface line of a width ranged between *0.7* to *~ 2.5 mm*. The joint's shear force reached a minimum and maximum value of *2000* and *2500 N*, respectively. The plunging depth was the most effective factor affecting the amount of the extruded aluminum and the joint's shear force.

Key words: AA6061, AISI 1006, friction spot joining, aluminum extrusion.

1. Introduction

Toxic emissions and fuel consumption can be minimized by using lightweight materials in structures of engineering applications [1]. By using low-weight materials such as aluminum alloys joined to and ferrous components weight savings can be accomplished [2]. Aluminum alloys are characterized by corrosion resistance, lightweight and high strength that make them used in ferrous structures. Hybridizing the aluminum alloys together with the steel requires suitable welding or joining techniques. Different welding techniques are used for welding the aluminum alloys with steel. The welding techniques occur by fusion the joint due to differences in melting point, cooling rate, and thermal and mechanical properties between the welded materials, which reduces the joint's efficiency [3]. Brittle intermetallic compounds are formed during the welding process, which weakens the joint's quality [4].

Welding of aluminum alloys with the steel structures has been carried out using various welding techniques, such as cold metal transfer [5], surface activated bonding [6], ultrasonic plus resistance spot welding (RSW) [7], laser penetration [8], barrel nitriding [9], friction welding [10], friction stir welding (FSW) [11], and friction stir spot welding (FSSW) techniques [12]. Nowadays, the most common techniques used in welding aluminum alloy with steel are FSW, FSSW, and RSW methods. The FSW is a solid-state technique [13], while the RSW is a fusion technique [14].

The FSSW technique is used for welding similar and dissimilar materials with a lap joint configuration by stirring the two materials with the aid of a rotating tool [15]. A steel alloy St-12 was welded with aluminum alloy AA5083 using the FSSW technique. A cross-section of the welded joint exhibited continuous and non-continuous intermetallic compounds (IMCs). The intermetallic compounds determined the mechanical properties of the joint [16]. The FSSW was used to weld aluminum alloy AA6063 with galvanized low carbon steel. Process parameters of the FSSW such as the rotating speed, plunging depth and design of rotating tool determine the joint's properties. Keyhole and hook formations were the main observation on the microstructure of the joint. Moreover, an IMC of Zn was formed at the interface line between the welded materials [17]. AC 170 PX aluminum alloy was welded together with T06 Z hot-dip galvanized steel using the FSSW. The welded materials

* To whom correspondence should be addressed

exhibited a formation of IMC of ZnO of a width of 0.68 μ*m* at the interface line of the welded materials. Microstructure of the fractured surface revealed the presence of inter-granular and cleavage brittle fractures [18].

On the other hand, RSW was used for welding the aluminum alloys with the steel by melting welded materials at a fusion zone under the tip of the RSW machine [19]. Different welding parameters and electrodes were used to weld AA6063-T6 to 16Mn high-strength steel using RSW. Microstructure examination indicated the formation of IMCs of type Fe-Al at the weld line of the welded materials, which reduced joint strength [20]. Mechanical properties, the failure mode of RSW of aluminum to steel depended on properties and dimensions of the IMCs layer. The thickness of IMCs is the most effective factor affecting mechanical properties and failure mode of welded materials [21]. Growth of IMCs during RSW of aluminum to steel was numerically simulated. The simulation indicated that the IMCs growth occurred over *900°C* [22]. Previous studies showed that the formation of IMCs, keyholes at the interface line of welded materials reduced the joint's strength. To prevent the formation of IMCs in welding of dissimilar materials, the friction spot joining (FSJ) technique was used to join materials without the formation of IMCs [23].

This work describes joining AA6061 together with pre-threaded carbon steel AISI 1006 using the friction joining technique. The joining process was carried out by a rotating tool by extruding aluminum metal through the pre-hole of the steel, with the aid of heat generation by friction between the tool and the aluminum. The effect of process parameters on joint performance was examined. The joining mechanism between the materials was investigated with the aid of microstructure examination.

2. Experimental setup

2.1. Materials and dimensions of specimens and tool

Two types of materials were used in this work to achieve the joining process: aluminum alloy AA6061 and carbon steel AISI 1006. The mechanical properties are listed in Table 1. The joining process was carried out by a non-consumable tool of a high-speed steel type (HSS).

Table 1. Mechanical properties of the materials.

Material	Reference	Tensile strength (*MPa*)	Yield strength (*MPa*)
AISI 1006	**ASTM**	***330***	***285***
	Measured	***337***	***294***
AA6061	**ASTM B209**	***289***	***241***
	Measured	***317***	***251***

The two materials specimens were prepared with a dimension of $25\times100\,mm^2$. The steel and aluminum specimens were *1.5* and *2 mm* thick, respectively. The steel specimens were machined with a hole of *5 mm* in diameter. The steel specimens hole was machined with an internal thread of M6 with *0.75* pitch, as shown in Fig.1. The tool was designed and manufactured with a shoulder diameter of *10 mm*, as shown in Fig.2.

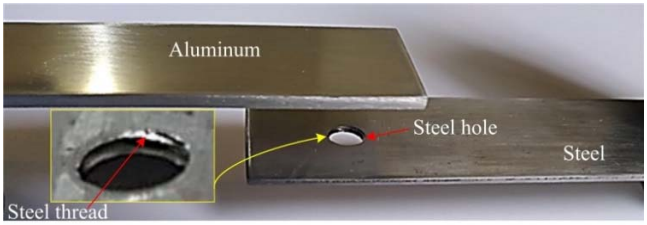

Fig.1. Steel and aluminum specimens.

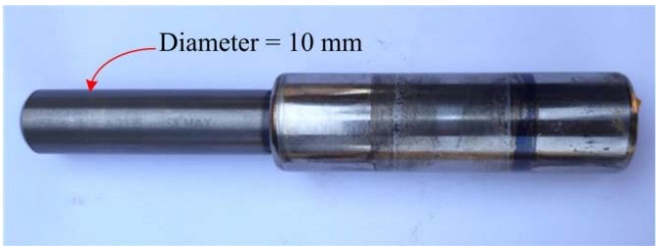

Fig.2. HSS tool dimension.

2.2. Process parameters

Three joining process parameters which affect the joint properties were taken into account, namely: preheating time, rotating speed and plunging depth of the tool. The main aim of the process is to heat the aluminum metal under the tool shoulder to a solid state and extrude it through the steel hole. The first two parameters (preheating time, rotating speed) generate frictional heat at the joint surface of the shoulder and aluminum specimen. In order to extrude the metal of the aluminum through the steel hole, an applied pressure of the rotating tool is required. So, the third parameter (plunging depth of the tool) was used to assess the extruding process. Values of those parameters affect the amount of heat generation and the extruded aluminum through the steel hole, affecting the joints' quality. So, for each parameter, three values were selected to study the effect of each parameter on the joint properties. The experiments were designed based on the design of the experiment's method (DOE). A Taguchi approach was used to design the levels of each parameter for each experiment. Table 2 lists the value of each parameter used for each joining experiment. According to the statistical analysis (Taguchi approach), sixteen experiments were designed with the aid of the Minitab software program.

Table 2. Taguchi design of joining process parameters.

Sample No.	1	2	3	4	5	6	7	8	9	10	11	12	13	14	15	16
Rotating speed (*RPM*)	*900*				*1120*				*1400*				*1800*			
Pre-heating time (*sec*)	*15*	*20*	*25*	*30*	*15*	*20*	*25*	*30*	*15*	*20*	*25*	*30*	*15*	*20*	*25*	*30*
Plunging depth (*mm*)	*0.15*	*0.30*	*0.45*	*0.60*	*0.30*	*0.15*	*0.60*	*0.45*	*0.45*	*0.60*	*0.15*	*0.30*	*0.60*	*0.45*	*0.30*	*0.15*

2.3. Friction spot joining process

The friction spot joining process was accomplished using a vertical milling machine with special fixtures to prevent the specimens from slipping during the process. The specimens' lap joint was put through the fixtures' internal slot, as shown in Fig.3a. The tool rotates and moves down until it reaches the upper surface of the aluminum specimens. For a specific time (pre-heating time), the tool stays in contact with the aluminum surface. At this stage, the aluminum specimen is heated and softened. The rotating tool penetrates the upper surface of the aluminum specimen with a particular plunging depth. The primary aim of this stage is to extrude the softened aluminum metal through the steel specimen hole with the aid of applied pressure during the plunging stage. The amount and characteristics of extruded aluminum depend on the pressure applied and generated heat by friction between the surface of the aluminum and the shoulder. Depending on the process parameters, the extruded metal can flow continuously until it meets the flat backup plate (lower die) of the machine base. On the other hand, the extruded aluminum can move transversally between the steel threads to fill the thread slot depending on the applied pressure. Figure 3b illustrates joined samples of aluminum and steel.

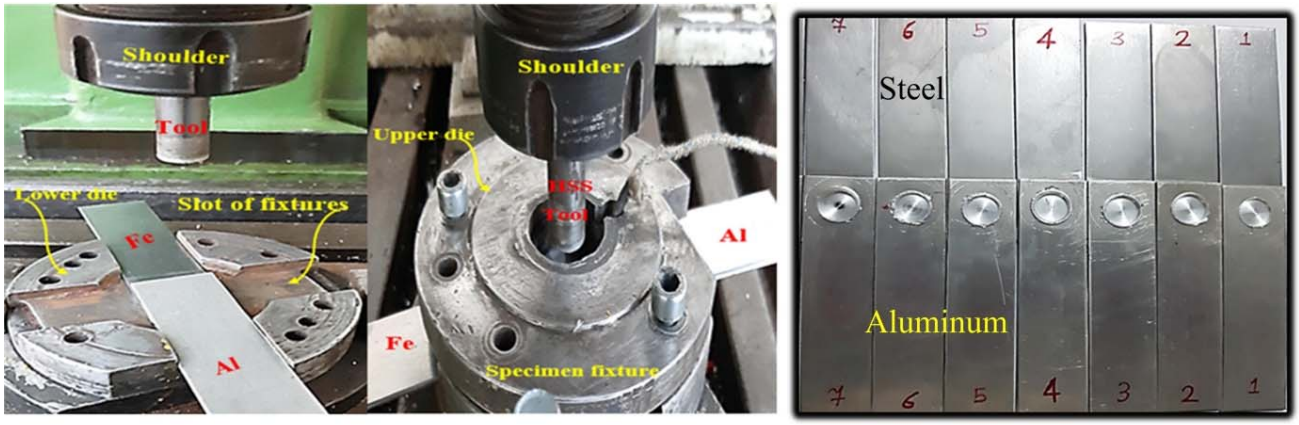

Fig.3. a) Lap joint configuration. b) Joined samples.

3. Results and discussion

3.1. Surface features of joints

Figure 4 shows the bottom view of the joined samples. Approximately all the joined samples indicated that the extruded aluminum fully filled the steel hole. This shows that the applied pressure and generated heat during the friction process were sufficient to extrude the aluminum with a uniform filling through the steel hole. Most of the joined samples exhibited the trace of the flat backup plate on the extruded aluminum metal due to high applied pressure and temperature [23]. Samples 1, 6, 11 and 16 exhibited a noticeable gap between the extruded aluminum and the inner surface of the steel hole compared with the other joined samples. Those samples were joined with the minimum plunging depth of the rotating tool (*0.15 mm*). Increasing the plunging depth of the tool resulted in decreasing the gap between the extruded aluminum and the inner surface of the steel hole, as shown in the samples of the highest plunging depth (sample No. 4, 7, 10 and 13). Those samples were joined with a maximum value of the plunging depth (*0.6 mm*). The operation of plunging was to apply a required pressure from the rotating tool on the aluminum specimen to extrude the heated aluminum through the steel hole. Increasing the plunging depth resulted in increased pressure, which led to the rise of the amount of extruded aluminum passing through the steel hole. So, the plunging depth of the tool has the greatest impact on the amount of extruded aluminum through the steel hole.

Fig.4. Extruded aluminum through steel hole.

3.2. Joint's shear force

The shear force test was carried out to investigate the mechanical properties of the joined materials at the lap joint region. The joined samples were tested by applying an axial force until they reached the final fracture. The shear force of the samples was recorded at the fracture point, representing the maximum shear force value during the shear test for each sample. This force can be considered as an ultimate value of shear force of the joint. This test revealed that the tested samples failed by shearing the extruded aluminum at the lap joint. Figure 5 illustrates a variation of the joint's shear for the joined samples. The recorded data indicated the shear force of the joints ranged from a minimum value of *2000 N* in samples No.1, 6, and 11 to a maximum value of *2500 N* in samples No.7 and 9. The samples of minimum shear force were joined with a minimum plunging depth of the tool (*0.15 mm*), while samples No. 7 and 9 were joined with a plunging depth of *0.6* and *0.45 mm*, respectively. This indicates that the joint's shear force has a significant effect on the plunging depth of the tool [24]. The first sets of the joined samples No.1, 2, 3 and 4 exhibited a uniform increase in the shear force, while the last group (samples No. 13, 14, 15 and 16) demonstrated a uniform decrease in the shear force. The first and last sets were joined by increasing and decreasing the plunging depth of the tool, respectively. With the small value of the plunging depth, a small amount of the aluminum metal can be freely extruded. A higher value of the plunging depth can result in applying a higher pressure on the extruded metal of the aluminum, which can assist in penetrating it through the inner threads of the steel hole and reducing the extruding defects. All of these factors can increase the joint's shear force.

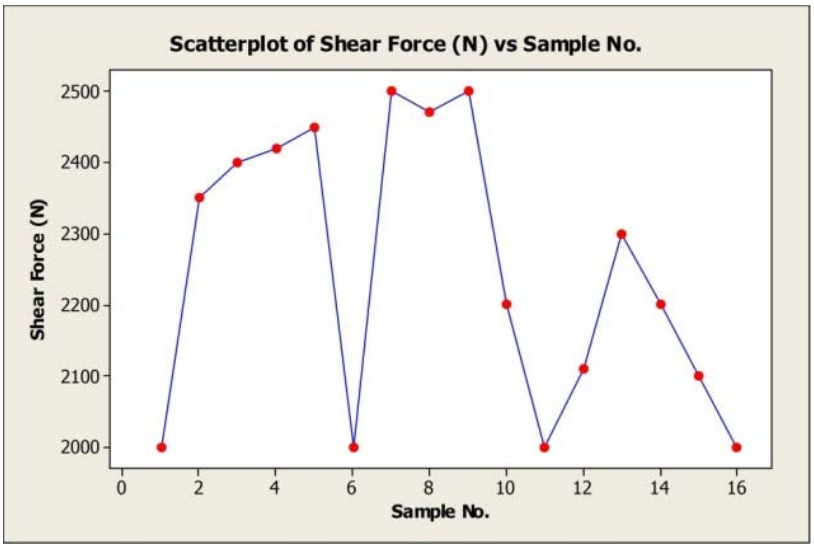

Fig.5. Joint's shear force of sample.

In order to explain the effect of the joining process parameters and process temperature on the joint's shear, the main effect was used by analyzing the experimental data, as shown in Fig.6. The maximum process temperature value was recorded for each sample. It ranged between a minimum value of *106.5°C* in sample No.1 and a maximum value of *169.6°C* in sample No.16. So, the samples were joined with a temperature (approximately) equal to a quarter of the melting point of the aluminum specimen. The results indicated that the increased rotating speed (more than *1120 RPM*) decreased the joint's shear force. Increasing the plunging depth of the tool increased the joint's shear force. The pre-heating time and process temperature exhibited a small or varying effect on the joint's shear force. This can be explained by the fact that the heating effect during the joining process has a small effect on the metallurgical properties of the extruded aluminum (the temperature reached *0.25 T* melting of the aluminum).

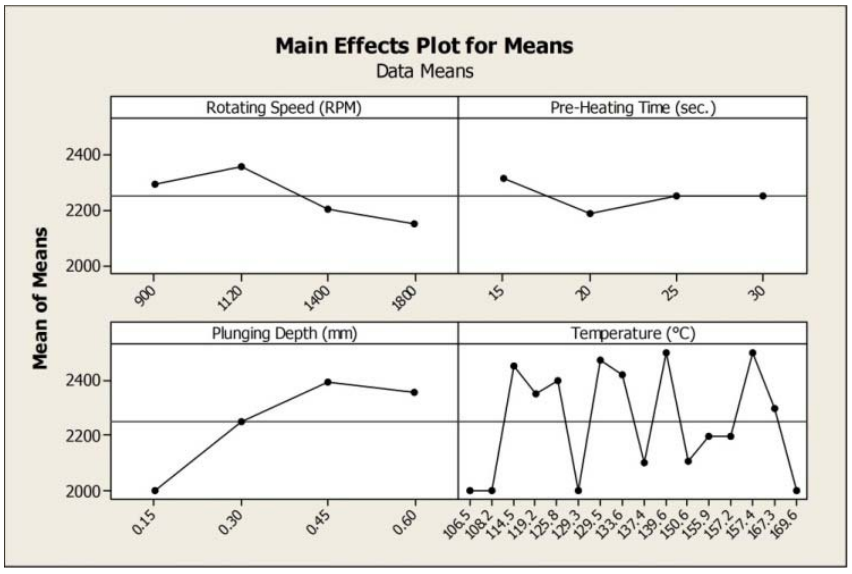

Fig.6. Main effect plot of joint's shear force.

Moreover, the Pareto chart shows that the plunging depth of the tool is the most influential factor followed by the rotating speed, process temperature and the pre-heating time, as shown in Fig.7.

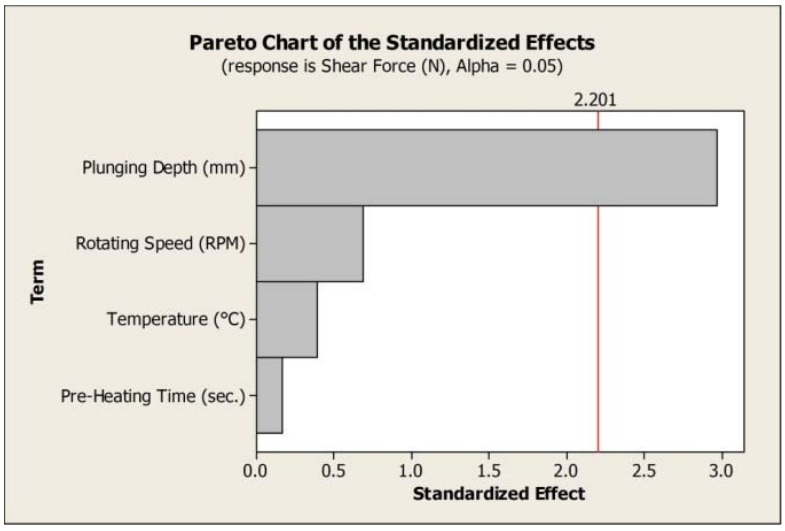

Fig.7. Pareto chart of joint's shear force.

Figure 8 illustrates the fractured surfaces of the joined samples at the aluminum and steel sides, respectively, for samples No. 2, 3, 7 and 8. The tested samples indicated that the joints failure was caused by two types of mode failure: shearing and pulling out the extruding aluminum. The aluminum metal was partially pulled out. It can be explained as follows. First, the second steel hole contained an extruded aluminum metal which acts as a cap-like rivet to resist the pullout of the aluminum. Secondly, the inner threads of the steel specimen, also resist the pullout of the aluminum metal from the steel hole. And finally, the mechanical interlock between the extruded aluminum and the inner surface of the steel hole. The joined samples exhibited the presence of part of the sheared aluminum on the steel specimen at its inner hole. This part of the aluminum resisted the pullout during the tensile test and is only sheared under the effect of the applied load during the

test. As a result, the effect of the stepped steel hole, steel threads and the mechanical interlock acted as factors to resist the joint pullout and improved the mechanical properties of the joints.

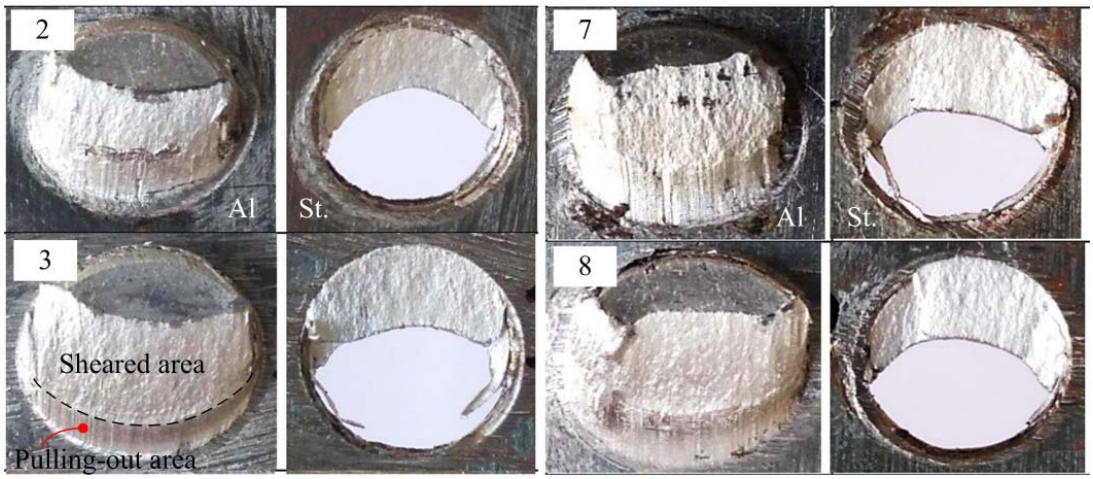

Fig.8. Fractured surfaces of joints.

3.3. Joint's macro-scope

During the joining process, the aluminum metal softens under the effect of heating process parameters. Softening of the extruded aluminum depends mainly on the process temperature. Two factors affect the process temperature: the rotating speed (*RPM*) and the preheating time (*t*). The preheating time will be the main factor in the process temperature for the same rotating speed value. For this case, increasing the softening-ability of the extruded aluminum depends on increasing the process temperature and/or the preheating time [25]. Figure 9a is a comparison of macroscopic images of joints cross-section joined with the same rotating speed and at different preheating time. It is observed that the joined samples with a higher preheating time (*30 sec*.) exhibited a smooth and full penetration of the extruded aluminum through the steel threads without deforming it. The joined samples with a smaller preheating time (*15 sec*.) exhibited a partial filling or penetration of the extruded aluminum through the steel threads, deforming the steel threads. When the preheating time is longer the process temperature rises, thus increases the softening-ability of the extruded aluminum. A higher softening of the extruded aluminum results in smooth penetration through the steel hole. During the penetration mechanism, the extruded aluminum exerts pressure on the steel thread. Samples No.4, 12 and 8 exhibited a smooth and full penetration of the extruded aluminum through the steel threads without deforming then. Samples No.1, 9, and 13 were joined with a short preheating time and/or process temperature. In this case, the extruded aluminum is not softened enough. A minor softening of the extruded aluminum reduces the penetration through the steel threads and increases the applied pressure from the extruded aluminum on the steel threads. So, the steel threads of samples No.1, 9, and 13 are highly deformed.

Two samples of maximum and minimum plunging depth were selected from each set of the rotating speeds to investigate the effect of the plunging depth (P) on the amount of extruded aluminum which penetrated the steel threads, as shown in Figure 9b. The images indicated that the higher plunging depth (*0.6 mm*) in samples No. 4, 7 and 10 resulted in a greater amount of extruded aluminum which penetrated the steel threads. A small amount of the extruded aluminum penetrating the steel thread was observed in samples No. 1, 6 and 11 due to a small plunging depth of the tool (*0.15 mm*). The samples of deep aluminum penetration exhibited a higher joint's shear force compared to those of small aluminum penetration.

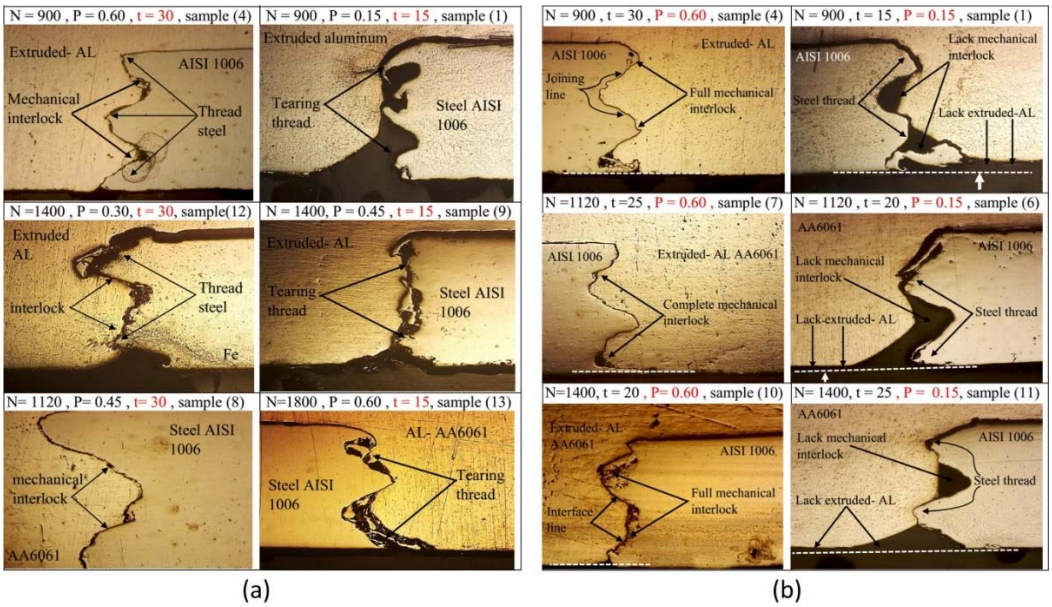

Fig.9. Joint's microscope: a) effect of pre-heating b) effect of plunging depth.

3.4. Joint's scanning electron microscopic and X-ray diffraction tests

Three samples (No. 4, 7 and 11) were selected to investigate the joining mechanism and the interface width between the two materials, with the aid of SEM examinations, as shown in Fig.10. The SEM results indicated that the joining between the two materials occurred by extruding the aluminum metal through the steel threads without the presence of defects such as voids, cracks or gaps. The extruded aluminum successfully penetrates pores (of micron size) of the inner surface of the steel hole. The two materials were joined by a micro-scale mechanical interlock mechanism between the extruded aluminum and the steel [26]. The interface line between the two materials is clearly observed. The width of the interface line ranged between (*0.7* to ~ *2.5*) µ*m*.

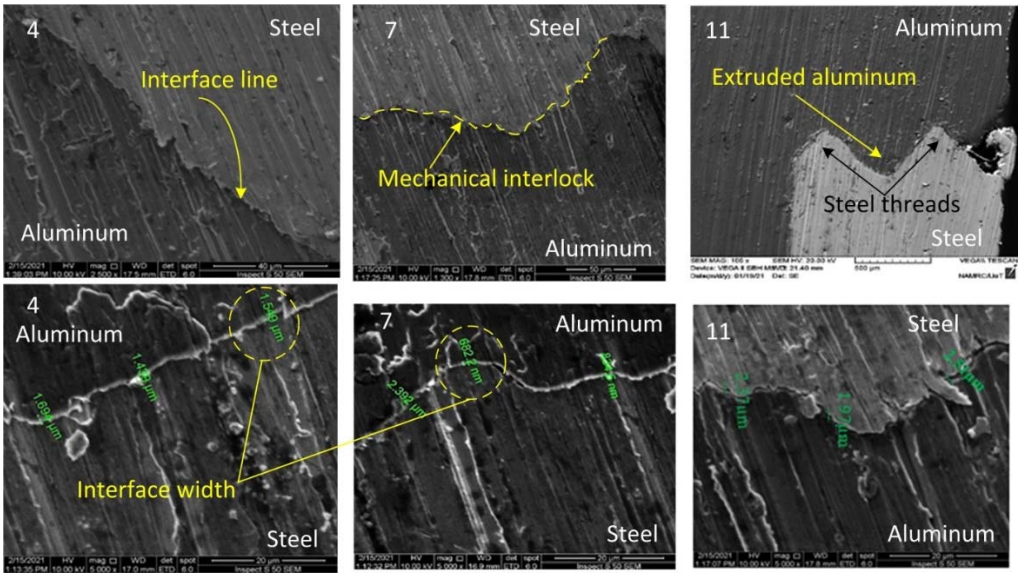

Fig.10. SEM of joint cross-section, samples No. 4, 7 and 11.

Moreover, the interface line between the joined materials was examined by X-ray diffraction tests for the sample 1 and 13, as shown in Fig.11.

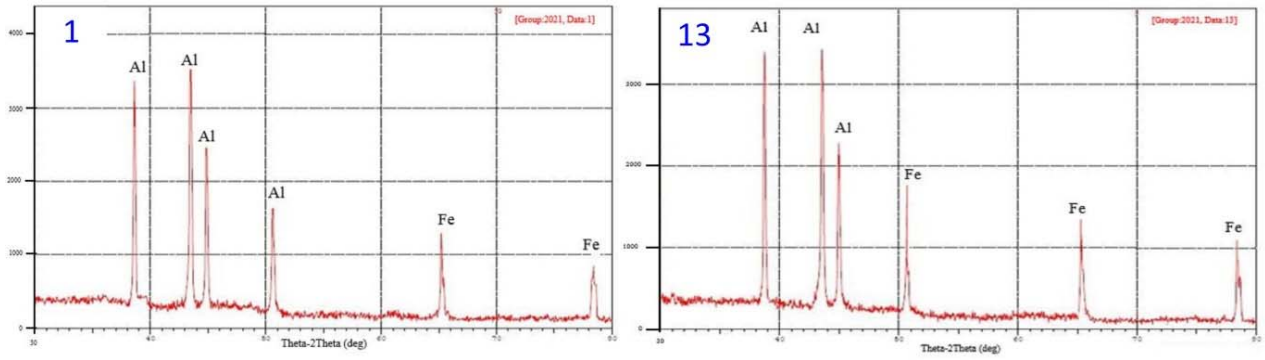

Fig.11. X-ray diffraction test, samples No. 1 and 3.

4. Conclusion

Aluminum alloy AA6061 was joined to a pre-holed and threaded carbon steel AISI 1006 by friction spot technique. The following conclusions can be drawn:

1) The two materials are joined by extruding the aluminum metal through the hole and the threads of the steel without visual gaps, voids or other defects.
2) A micro-scale mechanical interlock occurred between the joined materials at an interface line.
3) The plunging depth of the tool has the most significant effect on the amount of extruded aluminum through the steel hole.
4) The joined samples exhibited an ultimate shear force in the range of *2000-2500 N*.
5) The joint's shear force increased by increasing the plunging depth and decreasing the rotating speed of the tool, respectively.
6) The plunging depth of the tool has the strongest effect on the joint's shear force, followed by the rotating speed, process temperature and pre-heating time.
7) The joint failed by mixing two types of failure modes: shearing and pull-out of the extruded aluminum.
8) The compound effect of the mechanical interlock between the extruded aluminum and steel, stepped hole and threads of the steel specimen improved the mechanical properties of the joints.
9) Increasing the plunging depth and process temperature increased the penetration of the extruded aluminum through the steel threads.
10) The joint's shear force increased by increasing the penetration amount of the extruded aluminum through the steel threads.
11) Increasing the softening-ability of the extruded aluminum reduced the steel thread deformation and increased the joint's shear force.

Nomenclature

AA − aluminum alloy
AISI − American Iron and Steel Institute
°*C* − temperature degree (Celsius)
DOE − design of experiments
FSW − friction stir welding
FSSW − friction stir spot welding
HSS − high-speed steel

IMCs − intermetallic compoundsheat
mm − millimeter
MPa − megapascal
N − Newton
RPM − revolutions per minute
RSW − resistance spot welding
sec − second
SEM − scanning electron microscopic
t − time
Zn − zinc

References

[1] Amancio Filho S.T. and Blaga L.A. (Eds.) (2018): *Joining of Polymer-Metal Hybrid Structures: Principles and Applications*.– John Wiley & Sons.

[2] Abdullah I.T., Ridha M.H., Barrak O.S., Hussein S.K. and Hussein A.K. (2021): *Joining of Aa1050 sheets via two stages of friction spot technique*.– Journal of Mechanical Engineering Research and Developments, vol.44, No.4, pp.305-317.

[3] Huang J., He J., Yu X., Li C. and Fan, D. (2017): *The study of mechanical strength for fusion-brazed butt joint between aluminum alloy and galvanized steel by arc-assisted laser welding*.– Journal of Manufacturing Processes, vol.25, pp.126-133, https://doi.org/10.1016/j.jmapro.2016.11.014.

[4] Liu X., Lan S. and Ni J. (2014): *Analysis of process parameters effects on friction stir welding of dissimilar aluminum alloy to advanced high strength steel*.– Materials & Design, vol.59, pp.50-62, https://doi.org/10.1016/j.matdes.2014.02.003.

[5] Cao R., Yu G., Chen J.H. and Wang P.C. (2013): *Cold metal transfer joining aluminum alloys-to-galvanized mild steel*.– Journal of Materials Processing Technology, vol.213, No.10, pp.1753-1763, https://doi.org/10.1016/j.jmatprotec.2013.04.004.

[6] Howlader M.M.R., Kaga T. and Suga T. (2010): *Investigation of bonding strength and sealing behavior of aluminum/stainless steel bonded at room temperature*.– Vacuum, vol.84, No.11, pp.1334-1340, https://doi.org/10.1016/j.vacuum.2010.02.014.

[7] Lu Y., Mayton E., Song H., Kimchi M. and Zhang W. (2019): *Dissimilar metal joining of aluminum to steel by ultrasonic plus resistance spot welding-microstructure and mechanical properties*.– Materials & Design, vol.165, p.11, https://doi.org/10.1016/j.matdes.2019.107585.

[8] Chen S., Huang J., Ma K., Zhao X., and Vivek A. (2014): *Microstructures and mechanical properties of laser penetration welding joint with/without Ni-foil in an overlap steel-on-aluminum configuration*.– Metallurgical and Materials Transactions A, vol.45, No.7, pp.3064-3073, https://doi.org/10.1007/s11661-014-2241-1.

[9] Kong J. H., Okumiya M., Tsunekawa Y., Yun K.Y., Kim S.G. and Yoshida M. (2014): *A novel bonding method of pure aluminum and SUS304 stainless steel using barrel nitriding*.– Metallurgical and Materials Transactions A, vol.45, No.10, pp.4443-4453, https://doi.org/10.1007/s11661-014-2380-4.

[10] Matsuda T., Adachi H., Sano T., Yoshida R., Hori H., Ono S. and Hirose A. (2019): *High-frequency linear friction welding of aluminum alloys to stainless steel*.– Journal of Materials Processing Technology, vol.269, pp.45-51, https://doi.org/10.1016/j.jmatprotec.2019.01.023.

[11] Li S., Chen Y., Kang J., Amirkhiz B.S., and Nadeau F. (2019): *Friction stir lap welding of aluminum alloy to advanced high strength steel using a cold-spray deposition as an interlayer*.– Materials Letters, vol.239, pp.212-215, https://doi.org/10.1016/j.matlet.2018.12.060.

[12] Shen Z., Ding Y., Chen J., Amirkhiz B.S., Wen J.Z., Fu L. and Gerlich A.P. (2019): *Interfacial bonding mechanism in Al/coated steel dissimilar refill friction stir spot welds*.– Journal of Materials Science & Technology, vol.35, No.6, pp.1027-1038, https://doi.org/10.1016/j.jmst.2019.01.001.

[13] Leitao C., Arruti E., Aldanondo E. and Rodrigues D.M. (2016): *Aluminium-steel lap joining by multipass friction stir welding*.– Materials & Design, vol.106, pp.153-160, https://doi.org/10.1016/j.matdes.2016.05.101.

[14] Oliveira J.P., Ponder K., Brizes E., Abke T., Edwards P. and Ramirez A.J. (2019): *Combining resistance spot welding and friction element welding for dissimilar joining of aluminum to high strength steels*.– Journal of Materials Processing Technology, vol.273, p.10, https://doi.org/10.1016/j.jmatprotec.2019.04.018.

[15] Abdullah I.T. and Hussein S.K. (2018): *Improving the joint strength of the friction stir spot welding of carbon steel and copper using the design of experiments method*.– Multidiscipline Modelling in Materials and Structures, vol.14, pp.908-922, https://doi.org/10.1108/MMMS-02-2018-0025.

[16] Fereiduni E., Movahedi M. and Kokabi A.H. (2015): *Aluminum/steel joints made by an alternative friction stir spot welding process*.– Journal of Materials Processing Technology, vol.224, pp.1-10, https://doi.org/10.1016/j.jmatprotec.2015.04.028.

[17] Piccini J.M. and Svoboda H.G. (2015): *Effect of pin length on Friction Stir Spot Welding (FSSW) of dissimilar aluminum-steel joints*.– Procedia Materials Science, vol.9, pp.504-513, https://doi.org/10.1016/j.mspro.2015.05.023 .

[18] Dong H., Chen S., Song Y., Guo X., Zhang X. and Sun Z. (2016): *Refilled friction stir spot welding of aluminum alloy to galvanized steel sheets*.– Materials & Design, vol.94, pp.457-466, https://doi.org/10.1016/j.matdes.2016.01.066.

[19] Ghatei-Kalashami A., Zhang S., Shojaee M., Midawi A.R.H., Goodwin F. and Zhou N.Y. (2022): *Failure behavior of resistance spot welded advanced high strength steel: The role of surface condition and initial microstructure*.– Journal of Materials Processing Technology, vol.299, p.14, https://doi.org/10.1016/j.jmatprotec.2021.117370.

[20] Sun D., Zhang Y., Liu Y., Gu X. and Li H. (2016): *Microstructures and mechanical properties of resistance spot welded joints of 16Mn steel and 6063-T6 aluminum alloy with different electrodes*.– Materials & Design, vol.109, pp.596-608, https://doi.org/10.1016/j.matdes.2016.07.076 .

[21] Chen N., Wang H.P., Carlson B.E., Sigler D.R. and Wang M. (2017): *Fracture mechanisms of Al/steel resistance spot welds in lap shear test*.– Journal of Materials Processing Technology, vol.243, pp.347-354, https://doi.org/10.1016/j.jmatprotec.2016.12.015.

[22] Chen N., Wang M., Wang H.P., Wan Z. and Carlson B.E. (2018): *Microstructural and mechanical evolution of Al/steel interface with Fe2Al5 growth in resistance spot welding of aluminum to steel*.– Journal of Manufacturing Processes, vol.34, pp.424-434, https://doi.org/10.1016/j.jmapro.2018.06.024.

[23] Hussein S.K., Abdullah I.T. and Hussein A.K. (2019): *Spot lap joining of AA5052 to AISI 1006 by aluminium extrusion via friction forming technique*.– Multidiscipline Modelling in Materials and Structures, vol.15, pp. 1337-1351, https://doi.org/10.1108/MMMS-04-2019-0082.

[24] Kumar K.A. (2021): *Effect of tool plunge depth (TPD) on the microstructure and mechanical properties of FSW dissimilar joints reinforced with SiC nano particles*.– Materials Today: Proceedings, p.6, https://doi.org/10.1016/j.matpr.2021.09.056.

[25] Yu J., Zhao G., Cui W., Zhang C. and Chen L. (2017): *Microstructural evolution and mechanical properties of welding seams in aluminum alloy profiles extruded by a porthole die under different billet heating temperatures and extrusion speeds*.– Journal of Materials Processing Technology, vol.247, pp.214-222, https://doi.org/10.1016/j.jmatprotec.2017.04.030.

[26] Bergh T., Sandnes L., Johnstone D.N., Grong Ø., Berto F., Holmestad R., Midgley P.A. and Vullum P.E. (2021): *Microstructural and mechanical characterisation of a second generation hybrid metal extrusion & bonding aluminium-steel butt joint*.– Materials Characterization, vol.173, p.13, https://doi.org/10.1016/j.matchar.2020.110761.

Received: October 19, 2021
Revised: December 4, 2021